Integrating Pharmacokinetics and Network Analysis to Investigate the Mechanism of Moutan Cortex in Blood-Heat and Blood Stasis Syndrome

Qiuli Ye
Guangdong Pharmaceutical University
Ying Zhang
Jinan University College of Pharmacy
Donghui Yan
Guangdong Pharmaceutical University
Yue Sun
Guangdong Pharmaceutical University
Hui Cao
Jinan University College of Pharmacy
Shumei Wang
Guangdong Pharmaceutical University
Jiang Meng (jiangmeng666@126.com)
Guangdong Pharmaceutical University

Research Article

Keywords: Raw Moutan Cortex, UHPLC-DAD, absorbed compounds、pharmacokinetics, network analysis, HUVECs

Posted Date: May 31st, 2022

DOI: https://doi.org/10.21203/rs.3.rs-1655989/v1

Abstract

Background: Raw Moutan Cortex (RMC) has been used in China and other Asian countries for thousands of years. Its medical application is the treatment of cooling blood and promoting blood circulation; however, its therapeutic mechanism is still undefined.

Methods: In this study, the pharmacokinetics strategy that integrated network analysis was employed to explore the mechanism of RMC in blood-heat and blood stasis syndrome (BHS) model rats. Firstly, Ultra -High -Pressure Liquid Chromatography coupled with Diode Array Detector (UHPLC-DAD) method was developed to determine nine absorbed compounds in rat serum in BHS and normal rats after oral administration of RMC extract respectively. Then the pharmacology network was established based on the relationship between nine compounds absorbed into the blood and BHS targets. Finally, the predicted hub targets were validated experimentally in human umbilical vein endothelial cells (HUVECs).

Results: Pharmacokinetic study showed that the pharmacokinetic parameters of nine absorbed compounds had significant differences between BHS and normal groups($P<0.05$). Network analysis showed that 8 target genes, namely, F2, F10, F7, PLAU, MAPK14, MAPK10, AKT1, and NOS3 may be the primary targets regulated by RMC for the treatment of BHS. Among them, targets (F2, F10, F7 and MAPK14, MAPK10, AKT) and 4 active ingredients (paeonol, paeoniflorin, quercetin and oxypaeoniflorin) were selected for evaluating the reliability in vitro experiments, which revealed that the mechanism of RMC against BHS syndrome may inhibit inflammatory pathways and regulate coagulation cascades pathway for cooling and promoting blood circulation.

Conclusion: The proposed pharmacokinetics study integrated network analysis strategy provides a combination method to explore the therapeutic mechanism of RMC on BHS.

Background

Blood-heat and blood stasis syndrome (BHS) is a pathological condition in the blood circulation which may cause the development of various diseases, such as acute cerebral hemorrhage, stasis fever, coronary heart disease, etc. [1] Previous studies have shown that Chinese medicine for cooling blood and promoting blood circulation has anti-platelet aggregation, improve microcirculation, regulate immune function and anti-inflammatory. Definitely, its application prospects are broad [2, 3]. However, there are few research on the pharmacodynamic mechanism of most Chinese medicine for cooling blood and promoting blood circulation. Its active ingredients mechanism of action are still unclear, which are worthy of further investigation.

Raw Moutan Cortex (RMC) is the dried root bark of the Paeonia suffruticosa Andr Andr, as commonly traditional Chinese medicine for cooling and promoting blood circulation. It serves to clear heat and cooling blood, activates blood circulation and removing stasis, which commonly used in the clinical treatment of clearing excessive heat (typically manifesting in inflammation and related symptoms), amenorrhea and dysmenorrhea, traumatic injuries, carbuncles, ulcers and abscesses[4]. Modern pharmacological studies have shown that RMC extract could significantly inhibit the platelet aggregation rate induced by ADP, collagen and epinephrine, reduce the production of TXB2, inhibit platelet aggregation induced by collagen, adenosine diphosphate and arachidonic acid, significantly prolong TT and platelet aggregation time, and reduce platelet adhesion rate[4–9]. Besides, it was reported to exhibit a variety of biological activities, including anti-inflammatory[10–12], anti-oxidative effects[13, 14], anti-diabetes[15] and protective of myocardial ischemia[16].

The main chemical components of RMC are monoterpenes and their glycosides (such as paeoniflorin, oxypaeoniflorin, etc.), phenols and their glycosides (such as paeonol, etc.), flavonoids (such as quercetin), and et al.[17]. Its main components have been proven to have good anticoagulant, anti-inflammatory, improve microcirculation, and regulate immune functions [9, 18–20]. For example, quercetin, paeonol, paeoniflorin, oxypaeoniflorin and gallic acid have the effects of inhibiting platelet aggregation, anti-inflammation and anti-oxidation [8, 21–24]. In addition, 3,8-Dihydroxy-2-methylchromone can significantly extend APTT and promote blood circulation[25]. To date, most of the research on RMC have focused on the vitro studies, such as the chemical constituents and quantitative analyses, as well as quality control protocols[26–28]. However, there are few in-depth studies of the active components of RMC in vivo. In addition, these components absorbed into the BHS after oral administration in rats is still unknown. At present, only some monomer compounds (such as paeoniflorin and paeonol) have been reported in vivo[29, 30]. Further, traditional Chinese medicine mostly works in the mode of action of “multi-component, multi-target”. The single component

in vivo exposure value does not reflect the overall difference in the composition of Chinese medicine[31]. It is noteworthy that the active compounds, potential targets and pathways involved in these effects have not been systematically investigated.

From the perspective of pharmacokinetics, most traditional Chinese medicines are taken orally. Only when the traditional Chinese medicine ingredients are successfully absorbed into the blood and maintain a considerable concentration in the target organ can have the opportunity to exert their efficacy, which can provide a powerful evidence for determining the active compounds absorbed into the blood and deciphering their process in vivo [32, 33]. Network analysis is grounded in a nexus of interactions between drugs, targets and diseases. It is used to analyze the relationships between drugs, targets and diseases, while this method ignores whether the ingredients can be absorbed into the blood and its metabolism to play a curative effect, which may lead to unrealistic results [34, 35]. Therefore, in order to solve this problem, this paper proposes a pharmacokinetics and network analysis research strategy based on in vivo absorbed exposure. It lays the foundation for the search for potential active ingredients and provides a basis for revealing the mechanism of action of RMC in vivo. It also guides the clinical application of traditional Chinese medicine for cooling blood and provides a theoretical basis for activating blood under pathological conditions.

In this study, a high-efficiency and sensitive UHPLC-DAD method was used to determine the blood concentration of nine absorbed components in the serum of RMC in normal and BHS rats at different time point. The time-concentration curve was established and the relevant main pharmacokinetic parameters was obtained. Then, the pharmacology network was established based on the relationship between nine compounds absorbed into the blood and BHS targets. Finally, hub targets in the component–target network were experimentally validated in the human umbilical vein endothelial cells (HUVECs). Pharmacokinetic-based UHPLC-DAD combined with network analysis methods can provide a reliable and appropriate method for screening the potential active components of RMC for promoting blood circulation and removing blood stasis and elucidating its mechanism of action. The detailed process is shown in Fig. 1.

Methods

Chemicals and reagents

Raw Moutan Cortex pieces were bought from Guangzhou Zhixin Chinese Sliced Herbal Medicine Co. Ltd. (Guangzhou, China) and identified by associate professor Jizhu Liu (School of Traditional Chinese Medicine, Guangdong Pharmaceutical University). Voucher specimens were deposited at the Herbarium Centre, Guangdong Pharmaceutical University. The reference substances, including gallic acid, 5-hydroxymethylfurfural (5-HMF), oxypaeoniflorin, paeoniflorin, benzoic acid, methyl paraben, quercetin, paeonol, 3,8-dihydroxy-2-methylchromone, 3-hydroxy-4-methoxyacetophenone (IS) with purity ≥ 98%, were obtained from Chroma Biotechnology Co. Ltd. (Chengdu, China). Their chemical structures are shown in Fig. 2. Methanol and acetonitrile were HPLC grade (Oceanpak). Purified water was Watsons water. All other reagents used in this study were analytical grade. Nitrogen was purchased from Guangzhou Junduo Gas Company (purity > 99.9%) (Guangzhou, China). ELSA kit: thromboxane B2 (A002774), 6-keto-prostaglandin F1α (A0021984), Human coagulation factor II (FII)(A011227), Human coagulation factor Ⅶ (FⅦ) (A08571), Human coagulation factor X (FX)(A036278), all purchased from Shanghai Fusheng Industrial. RNAex Pro Reagent (AG11728, ACCURATE BIOTECHNOLOGY, HUNAN), EvoM-MLV RT Kit with gDNA Clean for qPCR (AG11728, ACCURATEBIOTECHNOLOGY, HUNAN).

Preparation of Moutan Cortex extract

The RMC pieces were soaked with 95% v/v ethanol at a solid-liquid ratio of 1:8 for 2 h, then reflux extracted for 2 h. After filtering, the residue was extracted again under the same conditions. The twice filtrates were collected and combined, and vacuum concentrated into an alcohol-free extractum. Last, the extractum was dissolved in water (equal to 6 g/ml of RMC) and stored in seal at 4°C.

Pharmacokinetic study

Twenty-four male Sprague-Dawley rats (weighing 300 ± 20 g) were purchased from Animal Experiment Center, Guangdong Academy of Medical Sciences (Certificate no. SCXK2013-0002). The rats were kept in an environmentally controlled breeding room at a temperature of 22 ± 2°C and a relative humidity of 55 ± 10% for 1 week before starting the experiments. They were fed with

standard laboratory food and water. Both the animal's care and the study protocol were conducted according to the National Institutes of Health Guide for the Care and Use of Laboratory Animals and followed the guidelines of the Ethics Committee of Guangdong Pharmaceutical University.

The rats were randomly divided into following four groups: normal groups (Normal groups), BHS model groups (BHS groups), normal group administrated with RMC water extraction (N-RMC group), BHS group administrated with RMC water extraction (BHS-RMC group), respectively. N-RMC group and BHS-RMC group rats were respectively orally administrated RMC water extraction (equal to 6 g/ml of RMC) for continuous 7 days at a dose of 10 ml/kg, once a day, one hour after the sixth day of administration. The rats in BHS groups and BHS-RMC group were subcutaneously injected with 10% aqueous suspension of yeast (10 ml/kg) and then subcutaneously injected with 0.1 mg/ml adrenaline hydrochloride solution twice (at a dose of 0.8 ml/kg, 4 hours apart) while body temperature remained relatively steady high. Those rats were soaked in ice-water for 5 min keeping their heads outside surface between two subcutaneous injections of adrenaline hydrochloride solution[36, 37]. At the same time, the normal groups and N-RMC group rats were injected with the same dose of saline (10ml/kg) subcutaneously. All rats were fasted for 12 h but free for water before taking the blood. On the seventh day, 0.3 ml blood samples were collected from fossa orbitalis vein at the time point of 0.083, 0.25, 0.5, 0.75, 1, 2, 3, 4, 6, 8, 10, 12 and 24 h after oral administration. All blood samples were immediately centrifuged at 12000 r/min for 10 min at 4°C and the serum samples were obtained and stored at -80°C until analysis.

Preparation of serum sample

Firstly, 100 μl serum was spiked with 10μL IS working solution to mix evenly, then 1ml methanol was added to protein precipitation, and centrifuged at 4000 r/min for 10 min at 4°C. Secondly, the supernatant was collected with a clean tube carefully and filtered through 0.22 μm microporous filter head. Thirdly, the filtrate was evaporated to dryness under a stream of nitrogen at 40°C. Finally, the residue was dissolved in 100 μl methanol and 10 μl of aliquot was injected into UHPLC -DAD system for analysis.

Instrument and Chromatographic conditions

The chromatography experiment was carried out using UPLC system (Thermo Fisher Scientific, USA). Chromatographic conditions: column: Acquity UPLC® BEH Shield RP_{18} Column (2.1mm × 100 mm, 1.7μm, Waters, USA). The column temperature was maintained at 30°C. mobile phase: Acetonitrile (A) and 0.4% (v/v) formic acid in water (B). The gradient conditions: 0–10 min, 5–15% A; 10–20 min, 15–35% A; 20–30 min, 35–95% A; 30–32 min, 95% A. The samples were kept at 4°C in the auto-sampler. flow rate: 0.2 mL/min; sample size: 2 μL; column temperature: 30°C. detection wavelength 254 nm.

Preparation of standards and quality control solutions

Primary stock solution of standards was prepared in methanol separately at concentrations of 2.075 mg/ml (gallic acid), 3.690 mg/ml (5-HMF), 0.640 mg/ml (oxypaeoniflorin), 1.125 mg/ml (3,8-dihydroxy-2-methylchromone), 2.235 mg/ml (paeoniflorin), 3.250 mg/ml (benzoic acid), 0.260 mg/ml (Methyl paraben), 2.385 mg/ml (quercetin), 0.482 mg/ml (paeonol) and 0.460 μg/ml (3-hydroxy-4-methoxyacetophenone, IS), respectively. Working standard solutions were prepared daily. All standard stock and working solutions were stored at 4°C.

Quality control (QC) samples were prepared by the same procedure to attain low, medium and high concentration levels. The concentrations were 186.75, 93.38 and 20.75 μg/ml for gallic acid; 405.90, 110.70 and 18.45 μg/ml for 5-HMF; 6.40, 3.20 and 0.96 μg/ml for oxypaeoniflorin; 129.38, 73.13 and 16.88 μg/ml for 3,8-dihydroxy-2-methylchromone; 145.28, 67.05 and 16.76 μg/ml for paeoniflorin; 243.75, 97.50 and 40.63 μg/ml for benzoic acid; 6.50, 3.90 and 1.30 μg/ml for methyl paraben; 715.50, 357.75 and 107.33 μg/ml for quercetin; 12.05, 7.23 and 2.41 μg/ml for paeonol.

Method validation

The selectivity of the method was evaluated by comparing the chromatograms of blank serum, blank serum spiked with the nine analytes and IS, serum samples of N-RMC and BHS-RMC rats administrated with RMC. Calibration standards of the mixture of nine components were prepared by spiking the standard mixture working solutions into 100 μl blank serum and 100 μl IS. The linearity of calibration curve was constructed by plotting the peak area ratios versus the concentration of nine components. The QC serum samples at three concentration levels were respectively analyzed in five replicates on the same day and on three consecutive validation days to evaluate the intra-day and inter-day precision and accuracy. The accuracy was expressed by the

percentage difference between amount spiked and determined while the precision was presented with the relative standard deviation (RSD%). The stability of nine components was evaluated to determine the changes in three different concentrations at low, medium and high levels of QC samples subjected to three different storage conditions. Short-term stability was evaluated by assessing QC samples at the room temperature (25°C) for 24 h. The freeze-thaw stability was inspected by implementing three freeze (-80°C) – thaw (room temperature, 25°C) cycles on consecutive days. Long-term stability was determined by storing at -80°C for 30 days. Extraction recovery was determined by calculating the peak area ratio of QC samples to corresponding post-extracted samples spiked with the analytes and internal standard at three concentrations of low, medium and high levels. The matrix effect was evaluated by comparison of the peak areas of nine components/IS in the post-extracted spiked samples and standard working solutions at the same concentration. The QC serum samples at three concentration levels were analyzed in five replicates, respectively.

The index of TXB2 and 6-Keto-PGF1 detect

It takes appropriate amount of serum and the levels of TXB2 and 6-Keto-PGFlα in the serum of rats in Normal group, BHS groups and BHS-RMC groups were detected by ELISA kit.

Statistical analysis

The concentrations of nine components of all samples were processed by PKSolver pharmacokinetics software. Statistical comparisons among groups were performed with GraphPad Prism 8 using a One-Way ANOVA analysis. Data expressed as mean ± SD and a P value ≤ 0.05 was considered to be statistically significant.

Network Analysis

Targets for nine compounds: the targets of nine compounds were predicted by

PharmMapper (http://lilab.ecust.edu.cn/pharmmapper/) limited to “Homo sapiens”; also including targets predicted from TCMSP (http://lsp.nwu.edu.cn/tcmspsearch.php). Subsequently, top 300 targets were predicted from the PharmMapper. Among the targets, those with z’-score > 0 was selected as the potential targets for the correlative ingredients. The PharmMapper online tool is a web server for potential drug target identification by reversed pharmacophore matching the query compound against anin-house pharmacophore model database[38].

Disease-related targets: By reviewing the literature on target proteins of traditional Chinese medicine for activating blood and cooling blood, it combined with RMC medicinal properties (bitter, acrid, slightly cold, homeward liver, kidney meridian), screen anti-inflammatory, improve hemodynamics, anti-coagulation, anti-platelet aggregation from TTD database equal to disease-related target protein. Finally, it locked the target proteins that may be related to activating blood and cooling blood[39–47].

PPI analysis

Screen for common targets at the crossover of compounds and diseases and import into the STRING database (https://string-db.org/, version 11.0), selecting "Homo sapiens" as the species source. The protein-protein interactions (PPIs) of proteins common to compounds and diseases targets were analyzed by String at the high confidence. The purpose of PPI was to get relevant targets, and to remove targets with low confidence.

Gene pathway analysis

Based on previous steps, compound-related targets and disease targets were prepared, and the drug-disease crossover genes were screened. Then, the Database for Annotation, Visualization and Integrated Discovery (DAVID, https://david.ncifcrf.gov/home.jsp, ver. 6.8) was used to identify the signal pathways and biological functions related to compound-disease target genes, which were analyzed by KEGG pathway enrichment ($p < 0.05$) and GO enrichment ($p < 0.05$).

Network construction

The compounds-target (C-T) and compounds-target -pathway network was built by network analysis software (Cytoscape 3.3.0).

Molecular docking

The molecular structures of the compounds were downloaded from PUBMED

(https://www.ncbi.nlm.nih.gov/) and then imported into Oppen Babel (2.4.1) software to transform the three-dimensional (3D) structure to mol2 file format. Several key targets are extracted from the major hub network, including F2, F7, F10, PLAU, MAPK14, MAPK10, AKT1 and NOS3. The 3D structures of Prothrombin(F2, pdb = 3tu7), Coagulation factor VII (F7, pdb = 5paw), Coagulation factor FX (F10, pdb = 3q3k), Urokinase-type plasminogen activator (PLAU, pdb = 1ejn), Mitogen-activated protein kinase 14 (MAPK14, pdb = 1a9u), Mitogen-activated protein kinase 10 (MAPK10, pdb = 3cgf), threonine-protein kinase(AKT1, pdb = 3ocb) and Nitric oxide synthase(NOS3, pdb = 1maj) were downloaded from the PDB database (https://www.rcsb.org/) (source: Homo sapiens; method: X-ray; resolution:> 1.5; number of ligands:> 1) using Sybyl-7.3 for processing. After removing the water molecules residues, hydrogenation, use the Surflex-Dock program Docking with its own ligand, the score obtained is used as the threshold value of the target. The compounds were docked with the target protein obtained by screening and scored. The target with a score greater than the target threshold (> 5) regarded as the master targets for RMC[48]. Then docking sites were analyzed using Discovery Studio 4.5 software to observe the Interaction between compound and target.

Cell Culture and Treatments

TNF-α was used to induce endothelial factor damage in Human Umbilical Vein Endothelial Cells (HUVEC) leading to inflammation and coagulation dysfunction. HUVECs were maintained in ECM complete growth medium (ECM, 5% FBS, 1%P/S and 1%EGCS). All cells were cultured at 37°C in a humidified atmosphere containing 5% CO_2. After three or four passages, the HUVECs were digested with 0.25% trypsin and seeded in a 6-well plate with a density of 1×10^5 cells/ml for ELISA analysis and RT-qPCR. First, we determined the effects of different doses of drug on the viability of HUVECs cells using the MTT methods(MTT results are shown in **Supplementary Fig. 1**).The cells used for experiment were divided into the following groups: control group (giving complete growth medium), model group (giving 25 ng/ml TNF-α), paeonol (50 ug/ml + 25 ng/ml TNF-α), paeoniflorin (500 ug/ml + 25ng/ml TNF-α), quercetin (1 ug/ml + 25 ng/ml TNF-α) and oxypaeoniflorin (500 ug/ml + 25 ng/ml TNF-α), for 8 h, respectively. Afterwards, take the supernatant and measure according to the ELISA kit, and detect the OD value at the wavelength of 450. Meanwhile, Total RNAs were extracted according to the manufacturer's instructions, which were used to generate cDNA using EvoM-MLV RT Kit with gDNA Clean for qPCR. ChamQTMUniversalSYBR qPCR Master Mix (Vazyme Biotech Co., Ltd, Q711-02) was performed on a Real-time PCR System. GAPDH was used as an internal control to normalize RNA expression. The primers information used in RT-qPCR were shown in Table 1.

Table 1
The primers used in RT-qPCR were shown in Table 1.

Primer	sequence (5' to 3')
GAPDH	F : ACGGATTTGGTCGTATTGG
	R : TCCCGTTCTCAGCCTTG
MAPK14	F : TTTGCTGGCTCTTGGAAC
	R : CGATCTCCCTGCACCTT
MAPK10	F : AGCAATAATCAGGCTTCCC
	R : TCATCAACCATCCACTTCC
AKT1	F : TGTGAAGGAGGGTTGGCT
	R : GCGCCACAGAGAAGTTGTT
F10	F : CGGCTACGACACCAAGC
	R : ACTTGAGGAAGGCGGTGA
F2	F : GCAAGCACCAGGACTTCA
	R : GAGGTCGCAGTACCCAAAG
F7	F: CTGAAGGCGGTTGTTTAGC
	R: GGAAGCAGGTGGGGAATA

Results

Method validation

As shown in Fig. 3, the nine components and IS was not detected in blank serum and could be well separated and detected in standards spiked serum and serum after oral administration of the RMC extract. The calibration curves of each target component displayed linearity over a range of concentration. The analytes had good linearity with correlation coefficients ($R2 \geq 0.9907$). The results indicated that the method was suitable for quantitative analysis of nine components and accorded with the pharmacokinetic requirements. (Table 2). The RSD values of precision test ranged from 0.76–9.97% for intraday assays and from 0.23–8.90% for interday assays. The accuracy ranged from 91.61–101.94% for all the QC levels of nine components (Table 3). The results of stability were in the range of 93.64% ~ 101.99% for short-term stability; 91.12% ~ 100.24% for freeze-thaw stability and 91.05% ~ 100.23% for long-term stability (Table 4). The extraction recovery was between 64.12% and 79.15% and matrix effect values ranged from 95.95–101.82% for all QC levels of nine components (Table 5). The results indicated that the precision, accuracy, stability and extraction recovery and matrix effect of the analytical method was acceptable in rat serum.

Table 2
Calibration curves, linear range of nine compounds.

Compounds	Calibration Curves	R^2	Linear range (μg/ml)	LLOQ (μg/ml)
5-HMF	Y = 0.0186x + 0.3545	0.9977	3.42 ~ 489.21	3.42
Gallic acid	Y = 0.0225x + 0.1842	0.9947	5.41 ~ 217.68	5.41
Oxypaeoniflorin	Y = 0.0181x + 0.2396	0.9939	0.58 ~ 11.89	0.58
Paeoniflorin	Y = 0.002x + 0.0016	0.9968	3.78 ~ 252.73	3.78
3,8-Dihydroxy-2-methylchromone	Y = 0.0228x + 0.0314	0.9980	3.39 ~ 164.31	3.39
Benzoic acid	Y = 0.0063x − 0.0248	0.9925	24.78 ~ 269.98	24.78
Methyl paraben	Y = 0.0858x + 0.0162	0.9915	0.15 ~ 8.04	0.15
Paeonol	Y = 0.0211x − 0.0143	0.9977	1.69 ~ 14.52	1.69
Quercetin	Y = 0.0502x − 1.6608	0.9907	107.66 ~ 895.54	107.66

Table 3
Intra-day and inter-day accuracy and precision of nine compounds in rat serum

Compounds	Spiked concentration(μg/ml)	Intraday			Interday		
		Measured concentration (μg/ml, mean ± SD)	Accuracy (%)	Precision RSD (%)	Measured concentration (μg/ml, mean ± SD)	Accuracy (%)	Precision RSD (%)
5-HMF	405.90	397.29 ± 1.45	97.88	1.23	398.09 ± 9.56	98.08	6.10
	110.70	102.22 ± 1.87	92.34	2.76	103.93 ± 2.20	93.88	5.42
	18.45	17.22 ± 1.36	93.33	3.45	17.25 ± 1.14	93.50	6.23
Gallic acid	186.75	181.97 ± 5.12	97.44	2.12	182.45 ± 4.20	97.70	1.23
	93.38	89.04 ± 3.45	95.35	2.56	90.96 ± 4.21	97.41	2.23
	20.75	19.01 ± 0.56	91.61	1.75	20.06 ± 0.52	96.67	1.23
Oxypaeoniflorin	6.40	5.93 ± 0.39	92.66	3.23	6.02 ± 0.24	94.06	1.89
	3.20	2.95 ± 0.18	92.19	1.85	2.98 ± 0.12	93.13	2.21
	0.96	0.89 ± 0.02	92.71	0.76	0.91 ± 0.36	94.79	3.89
Paeoniflorin	145.28	138.74 ± 3.85	95.50	5.45	139.29 ± 6.42	95.88	3.25
	67.05	65.78 ± 1.59	98.11	4.52	66.68 ± 2.23	99.45	3.45
	16.76	16.00 ± 0.81	89.50	4.05	15.76 ± 0.87	94.03	6.21
3,8-Dihydroxy-2-methylchromone	129.38	123.71 ± 1.08	95.62	1.92	125.30 ± 1.63	96.85	2.23
	73.13	67.71 ± 0.24	92.59	0.63	69.49 ± 0.36	95.02	0.23
	16.88	15.04 ± 0.15	95.02	2.12	15.12 ± 2.18	89.57	6.71
Benzoic acid	243.75	234.56 ± 2.25	96.23	1.12	136.39 ± 3.67	100.95	3.64
	97.50	93.56 ± 2.43	95.96	3.30	96.66 ± 2.73	99.14	3.12
	40.63	38.04 ± 0.25	93.63	4.93	39.01 ± 0.62	96.01	5.12
Methyl paraben	6.50	6.29 ± 0.19	96.77	3.29	6.23 ± 0.18	95.85	1.01
	3.90	3.60 ± 0.05	92.31	1.55	3.71 ± 0.13	95.13	3.12
	1.30	1.21 ± 0.02	93.08	8.82	1.21 ± 0.02	93.08	1.23
Paeonol	12.05	11.48 ± 1.37	95.27	4.48	11.37 ± 0.23	94.36	1.02
	7.23	6.88 ± 0.33	95.16	2.04	6.63 ± 2.23	91.70	1.09
	2.41	2.25 ± 0.17	93.36	7.95	2.36 ± 0.18	97.93	2.90
Quercetin	715.50	698.61 ± 15.88	97.64	3.80	693.58 ± 11.45	101.94	8.90
	357.75	347.97 ± 2.45	97.27	1.21	349.95 ± 8.23	97.82	3.09
	107.33	101.28 ± 1.89	94.36	9.97	102.39 ± 1.64	95.40	3.32

Table 4
Stability of nine compounds in rat serum (mean ± SD, n = 5).

Compounds	Spiked Concentration (μg/ml)	Short-term stability (%)	Freeze-thaw stability (%)	Long-term stability (%)
5-HMF	405.90	98.49 ± 2.33	92.50 ± 1.32	91.05 ± 1.21
	110.70	96.62 ± 2.12	95.44 ± 2.21	95.2 9 ± 4.89
	18.45	97.06 ± 3.20	96.33 ± 2.31	95.24 ± 2.01
Gallic acid	186.75	94.25 ± 1.41	93.00 ± 1.25	93.26 ± 1.52
	93.38	97.26 ± 1.56	96.72 ± 1.63	95.73 ± 2.42
	20.75	98.70 ± 2.56	98.02 ± 3.02	100.23 ± 2.30
Oxypaeoniflorin	6.40	97.81 ± 1.33	95.51 ± 2.14	93.42 ± 2.41
	3.20	97.86 ± 2.02	96.22 ± 2.31	96.23 ± 4.30
	0.96	98.45 ± 1.07	98.54 ± 3.32	97.41 ± 2.75
Paeoniflorin	145.28	93.88 ± 3.16	91.12 ± 3.88	58.83 ± 1.56
	67.05	95.55 ± 2.89	94.39 ± 1.02	95.19 ± 2.40
	16.76	97.66 ± 3.56	95.27 ± 0.75	96.05 ± 3.15
3,8-Dihydroxy-2-methylchromone	129.38	101.99 ± 0.28	100.24 ± 2.23	100.14 ± 2.04
	73.13	94.32 ± 2.63	95.21 ± 1.86	97.52 ± 1.56
	16.88	98.79 ± 2.30	96.15 ± 1.38	93.29 ± 3.22
Benzoic acid	243.75	95.72 ± 3.71	93.60 ± 0.86	91.69 ± 1.02
	97.50	96.05 ± 4.02	92.39 ± 2.01	91.24 ± 4.23
	40.63	96.83 ± 5.63	92.18 ± 2.62	88.94 ± 1.21
Methyl paraben	6.50	93.64 ± 1.93	90.19 ± 2.20	99.94 ± 1.26
	3.90	99.13 ± 1.23	99.11 ± 1.28	98.14 ± 1.23
	1.30	99.09 ± 7.25	98.91 ± 4.19	94.26 ± 2.36
Paeonol	12.05	100.63 ± 2.38	100.02 ± 2.16	98.12 ± 4.12
	7.23	96.10 ± 3.02	95.16 ± 2.07	94.40 ± 2.09
	2.41	98.96 ± 2.00	97.06 ± 2.17	92.82 ± 5.85
Quercetin	715.50	96.69 ± 1.54	95.36 ± 1.22	94.59 ± 2.51
	357.75	97.53 ± 5.23	96.40 ± 1.24	95.53 ± 0986
	107.33	99.63 ± 3.20	98.04 ± 3.55	98.65 ± 2.20

Table 5
Extraction recovery and Matrix effect of nine compounds in rat serum (mean ± SD, n = 5)

Compounds	Spiked Concentration (μg/ml)	Extraction recovery(%)	RSD(%)	Matrix effect(%)	RSD(%)
5-HMF	405.90	79.15 ± 1.15	10.81	99.65	6.27
	110.70	76.29 ± 1.53	6.92	99.26	9.15
	18.45	75.22 ± 1.22	7.55	98.00	5.76
Gallic acid	186.75	74.82 ± 1.00	6.74	97.18	5.76
	93.38	72.41 ± 0.55	2.46	99.91	5.82
	20.75	68.64 ± 1.51	2.25	100.01	2.91
Oxypaeoniflorin	6.40	72.37 ± 2.13	12.38	97.62	9.27
	3.20	72.93 ± 0.82	6.15	101.21	5.75
	0.96	76.42 ± 1.09	3.45	98.56	5.65
Paeoniflorin	145.28	66.76 ± 1.55	3.65	99.55	9.56
	67.05	64.20 ± 1.22	11.12	99.17	8.60
	16.76	65.89 ± 2.56	12.55	99.15	2.59
3,8-Dihydroxy-2-methylchromone	129.38	75.97 ± 1.23	3.12	98.43	3.42
	73.13	74.48 ± 1.99	9.46	98.21	7.29
	16.88	72.12 ± 1.22	5.76	99.94	5.28
Benzoic acid	243.75	75.88 ± 1.89	10.27	97.45	5.21
	97.50	74.56 ± 2.71	3.21	97.18	7.72
	40.63	69.82 ± 4.91	9.11	98.92	7.65
Methyl paraben	6.50	77.08 ± 1.84	11.30	97.78	9.98
	3.90	75.26 ± 1.24	9.99	98.42	5.23
	1.30	78.88 ± 3.47	8.13	95.95	3.50
Paeonol	12.05	68.76 ± 0.91	7.92	98.97	5.20
	7.23	64.12 ± 2.87	3.01	98.32	6.76
	2.41	65.87 ± 1.96	7.71	101.20	5.28
Quercetin	715.50	67.62 ± 0.71	10.27	98.96	11.11
	357.75	66.35 ± 1.71	4.95	99.80	9.04
	107.33	65.45 ± 1.67	7.89	98.81	2.24

The TXB2 and 6-Keto-PGF1 in Normal and Model Rats

The concentrations of TXB2, 6-Keto-PGFIα and TXB2/6-Keto-PGFIα of the serum in each group rats at the same time point are shown in Fig. 4. The results demonstrated that the 6-Keto-PGFIα value was lower in the BHS model rats comparing to the normal rats after 0.5h in Fig. 4**(A)**, while the TXB2 and TXB2/6-Keto-PGF1 value was higher in the BHS model rats than normal rats in Fig. 4**(B, C)**, which implied the BSH model was successful. After oral administration with the RMC extract, it showed a higher level of 6-Keto-PGF1 and a lower level of TXB2 and TXB2/6-Keto-PGF1 in BSH-RMC group as compared with BSH group, and infinitely approaching to the normal group, which confirmed that RMC had a good therapeutic effect on BHS rat.

Pharmacokinetic study

The proposed method was successfully applied to the pharmacokinetic study in BHS groups and normal groups rats after oral administration with the RMC extract. The pharmacokinetic parameters were calculated according to the non-compartmental model. The concentration-time profile of the nine components is illustrated in Fig. 5 and the main pharmacokinetic parameters and significant differences among each group were presented in Table 6. After comparing the pharmacokinetic data of the BHS groups and normal groups rats, it could be concluded that there were significant differences between the pharmacokinetic parameters, such as AUC, Cmax, CL / F ($p < 0.05$).

Table 6
The pharmacokinetic parameters of nine components of RMC extracts between N-RMC and BHS-RMC group (n = 6)

Analyte	Group	Pharmacokinetics parameters					
		$T_{1/2}$ (h)	T_{max} (h)	C_{max} (μg/ml)	AUC (μg/ml*h)	MRT (h)	CL/F (ml/min/kg)
Gallic acid	N-RMC	10.76 ± 0.87	0.75 ± 0.00	126.96 ± 2.90	1018.73 ± 26.63	17.30 ± 0.80	58.93 ± 1.58
	BHS-RMC	6.33 ± 0.45↓	1.00 ± 0.00↑	180.13 ± 11.06↑	1067.98 ± 72.88↑	10.02 ± 0.96↓	56.40 ± 3.79↓
5-HMF	N-RMC	3.20 ± 0.03	3.00 ± 0.00	413.25 ± 2.01	1563.50 ± 4.63	4.55 ± 0.03	38.38 ± 0.11
	BHS-RMC	7.33 ± 2.10↑	0.75 ± 0.00↓	111.37 ± 7.25↓	740.76 ± 20.26↓	7.47 ± 0.48↑	81.05 ± 2.25↑
Oxypaeoniflorin	N-RMC	3.08 ± 0.98	4.00 ± 0.00	10.23 ± 0.11	45.72 ± 1.4	5.53 ± 0.50	1313.57 ± 40.19
	BHS-RMC	15.13 ± 2.25↑	0.50 ± 0.00↓	2.09 ± 0.04↓	24.16 ± 3.09↓	21.59 ± 3.42↑	2519.95 ± 343.95↑
3,8-Dihydroxy-2-methylchromone	N-RMC	4.73 ± 0.29	0.75 ± 0.00	115.71 ± 2.12	660.32 ± 29.92	6.90 ± 0.68	91.01 ± 4.00
	BHS-RMC	19.01 ± 1.78↑	0.75 ± 0.00	134.00 ± 3.26↑	756.93 ± 8.72↑	14.06 ± 1.07↑	79.28 ± 0.92↓
Paeoniflorin	N-RMC	9.75 ± 0.47	0.50 ± 0.00	201.57 ± 1.86	1449.69 ± 62.31	15.53 ± 0.94	41.45 ± 1.78
	BHS-RMC	3.60 ± 0.31↓	0.75 ± 0.00↑	84.23 ± 1.99↓	298.12 ± 7.60↓	5.06 ± 0.22↓	201.37 ± 5.16↑
Benzoic acid	N-RMC	11.11 ± 1.88	4.00 ± 0.00	143.65 ± 4.48	1877.15 ± 216.74	16.96 ± 2.76	32.30 ± 3.70
	BHS-RMC	10.04 ± 0.67↓	3.00 ± 0.00↓	212.92 ± 5.26↑	2319.78 ± 71.29↑	13.26 ± 0.79↓	25.88 ± 0.80↓
Methylparaben	N-RMC	4.93 ± 0.23	0.75 ± 0.00	6.35 ± 0.53	22.82 ± 1.34	7.91 ± 0.56	2636.68 ± 156.55
	BHS-RMC	17.91 ± 0.84↑	1.00 ± 0.00↑	2.16 ± 0.11↓	39.87 ± 1.34↑	27.07 ± 1.16↑	1506.43 ± 50.68↓
Quercetin	N-RMC	9.97 ± 0.35	4.00 ± 0.00	643.27 ± 19.81	7338.63 ± 165.50	16.64 ± 0.56	8.18 ± 0.18
	BHS-RMC	15.49 ± 0.54↑	4.00 ± 0.00	739.851 ± 4.17↑	10036.28 ± 171.6↑	20.45 ± 0.66↑	5.98 ± 0.10↓
Paeonol	N-RMC	7.84 ± 0.08	0.75 ± 0.00	11.76 ± 0.13	106.52 ± 1.23	12.11 ± 0.17	563.34 ± 6.49
	BHS-RMC	4.37 ± 0.15↓	0.75 ± 0.00	10.37 ± 0.23↓	45.54 ± 0.83↓	4.63 ± 0.12↓	12450.58 ± 8613↑

"" indicates that there is a significant difference between the N-RMC and the BHS-RMC ($P < 0.05$), and "" indicates that the N-RMC and the BHS-RMC are significantly different ($P < 0.01$), ↑was represented rising in BHS-RMC comparing N-RMC, ↓ was represented declining

Network analysis

As a result, 169 targets of nine absorbed compounds were summarized. Meanwhile, it locked the 213 targets associated with blood-heat and blood stasis syndrome (BHS) (Fig. 6A). Then the overlapping targets were screened from the compound related targets and BHS related targets. Finally, 23 proteins common to compounds and diseases targets were analyzed by PPI (Fig. 6B) (STRING: functional protein association networks) with the score at the high confidence, which identified as potential targets of RMC for treating BHS Syndrome were imported into Cytoscape 3.2.1 for analysis.

A network was constructed to display the compounds–targets interactions (Fig. 6C). As can be seen from the Figure, compounds (paeonol, paeoniflorin, quercetin, oxypaeoniflorin, gallic acid, methyl paraben and 3,8-Dihydroxy-2-methylchromone) were shared by 23 proteins that contribute to the regulation of BHS syndrome and may be the active ingredients in RMC to exert therapeutic effects. Key targets and main components are extracted from the major hub network by defining nodes with degrees higher than the average number of neighbors. Among the 23 proteins, 8 proteins, namely, F2, F10, F7, MAPK14, MAPK10, AKT1, NOS3, PLAU and 7 compounds, such as paeonol, paeoniflorin, quercetin, oxypaeoniflorin, gallic acid, methyl paraben and 3,8-Dihydroxy-2-methylchromone were found to have the highest degree values, which may be the key treatment targets and active ingredients of RMC for treatment of BHS (Table 7).

Table 7
The topological parameters of components and key targets

Name	Degree	Betweenness Centrality	Closeness Centrality
Oxypaeoniflorin	21	0.56313	0.731707
Paeoniflorin	16	0.260056	0.588235
F7	6	0.110326	0.535714
MAPK14	5	0.093949	0.5
Gallic acid	4	0.072506	0.379747
MAPK10	4	0.059543	0.5
F2	5	0.045091	0.5
NOS3	4	0.030639	0.483871
AKT1	3	0.022278	0.405405
Methyl paraben	4	0.017795	0.4
PLAU	3	0.017271	0.46875
3,8-Dihydroxy-2-methylchromone	5	0.014472	0.38961
F10	3	0.010943	0.46875
PPARG	3	0.010943	0.46875
Quercetin	4	0.009219	0.38961
Paeonol	3	0.005351	0.379747

Based on 23 potential targets, we performed GO and KEGG enrichment analysis. Enrichment of the KEGG pathway could be divided approximately into modules of cancer, anticoagulant and inflammation. (Fig. 6C). In the GO enrichment analysis (Fig. 6E), 23 proteins are mainly involved in the regulation process of transcription factors, which indicated that numerous biologic processes were involved in BHS treatment.

Computer-aided interactive molecular docking can be used to predict and analyze the structure-activity relationship between receptor and ligand. The ingredients chosen for molecular docking were based on their high contents analyzed by pharmacological activities screened by network pharmacology. According to the evaluated index of the Surflex-Dock program, the compound has a strong affnity with the target protein when the scoring of binding force is > 5.0. As can be seen from Fig. 7A, 4 compounds (paeonol, paeoniflorin, quercetin, oxypaeoniflorin) were blinding with 8 hug targets (score > 5), which may be the

potential active ingredients of RMC. Among them, F2 and MAPK14 were selected as coagulation and inflammation targets to explore their possible binding interactions. The formation of hydrogen bonds involving the oxygen and the C = O group of the ring, which also makes a contribution to binding. As showed in Fig. 7 **(**depicted in **supplementary Table 1)**, in the structure of thrombin (F2), quercetin can form a strong conventional hydrogen bond with PHE227, GLU192 and SER195. Additionally, the critical catalytic triads Ser195 were located in the middle of the active site (Fig. 7B). Paeoniflorin has four direct H-bonds to GLY216, GLY219, CYS220 and GLU192(Fig. 7C). The docked pose of paeonol within MAPK14 showing key hydrogen bond interaction with ASP168 and MET109 (Fig. 7D). Quercetin showing hydrogen bond interaction with ASP168 and LEU104(Fig. 7E). Compounds showed different hydrogen bonds to the same target, which is due to the different structures of the compounds. Conversely, the binding pattern and alignment of Paeoniflorin and oxypaeoniflorin were found very similar to co-crystal ligand in the binding site because of the similar structure. As can be seen from Fig. 7F-G, Paeoniflorin is bonded with PHE169 and LYS53, whereas the same interaction was also recognized with oxypaeoniflorin.

Targets Validation

In order to further assess the obtained results in systems pharmacology analysis, we have examined the compound potential activating blood and anti-inflammatory using HUVECs cells induced by TNF-α (25 ng/ml). In particular, we conduct ELISA kit and RT-qPCR analysis for hug targets such as F2, F7 and F10 protein expression to confirm activating blood effects of the 4 compounds (paeonol, paeoniflorin, quercetin and oxypaeoniflorin), as well as RT-qPCR analysis for AKT1, MAPK14 and MAPK10 predicted anti-inflammatory effects of those 4 compounds. As shown in Fig. 8, the levels of F2, F7and F10 protein in the panel of HUVECs cell lines tested are reported (Fig. 8A-F). We observed that the protein expressions of F2, F7and F10 protein in HUVECs cells are significantly declined after the treatment of paeonol, quercetin, paeoniflorin and oxypaeoniflorin (excepting oxypaeoniflorin has no effect on F2). Simultaneously, a significant decrease in MAPK14 and MAPK10 mRNA expression was observed after the treatment of those 4 compounds **(**Fig. 8H-I**).** Among them, only oxypaeoniflorin could decrease the expression of AKT (Fig. 8G**)**. These data support the in vitro study that the docking prediction is in line with the validated detection by ELISA and RT-PCR, indicating high reliability of our docking.

Discussion

TXB2 and 6-Keto- PGFIα are commonly used as vivo indexes in studying the drug hemostasis mechanism. The values of TXB2, 6-Keto-PGFIα and TXB2/6-Keto-PGFIα between BHS and Normal group, BHS-RMC and BHS model group are significantly different ($p < 0.05$). The TXB2 and TXB2/6-Keto-PGFIα value of the BHS model group are higher than normal group, while the 6-Keto-PGFIα value is lower in normal group after 0.5h, which indicated that the BHS model is successful. However, after administration, BHS-RMC group showed lower level of TXB2 and TXB2/6-Keto –PGFIα and higher level of 6-Keto-PGFIα as compared to BHS model group. Simultaneously, there was no significant difference between the normal group and BHS-RMC group (Fig. 4). The results showed that RMC has a better therapeutic effect on BHS syndrome and can correct the pathological state to be close to the normal state.

The 9 components were measurable in plasma after oral administration RMC extract. The nine compounds pharmacokinetics parameters varied in normal and BHS rats considerably (Table 6), which revealed that the pathological state could influence the pharmacokinetic characteristics of compounds. The AUC and C_{max} of 3, 8-dihydroxy-2-methylchromone, benzoic acid, quercetin and gallic acid in BHS-RMC were greater than N-RMC (AUC increased by 15%, 23%, 36%, 5% and 74%; C_{max} increased by 16%, 49%, 15% and 42%respectively), while their CL / F value is significantly lower, which indicated that these four components had the higher exposure and bioavailability as well as slower elimination rate in BHS rats than normal rats. In contrast, 5-HMF, oxypaeoniflorin, paeoniflorin, and paeonol showed smaller AUC0-t and Cmax in BHS-RMC group, while CL/F value increased. Significantly, it indicated that these four components showed lower exposure and bioavailability as well as fast metabolism in BHS-RMC as compared to those in N-RMC, which revealed that the pathological state could influence the pharmacokinetic characteristics of compounds.

In addition, it was noticeable that oxypaeoniflorin was not detected in BHS-RMC rats after 6h. (**Figure. 5**). Similarly, paeonol and paeoniflorin are not detected after 8h and 12h, respectively, which indicated that pathological state accelerated the metabolic process of the drug, resulting changes in the body's absorption, distribution, metabolism and excretion of these three components.

It was also found that the plasma profile of paeonol presented bimodal (double peak) phenomenon after oral administration of RMC extract in both normal and model rats, which are consistent with those reported in the literature[49, 50]. According to reports, paeonol had a strong first-pass effect, metabolized and excreted quickly in the body, which resulted in low bioavailability. Furthermore, the bioactivity of paeonol metabolites that had been confirmed has pharmacological activity, which suggested that the absorption and paeonol were accelerated under pathological conditions, and its metabolites were quickly absorbed into the blood to play a therapeutic role[50, 51]. As for paeoniflorin and oxypaeoniflorin, studies had shown that they were generally enzymatically hydrolyzed into aglycones by intestinal flora to exert their therapeutic effects, which suggested that the intestinal flora had changed under the pathological state, thereby accelerating the metabolism of paeoniflorin and oxypaeoniflorin into aglycones to quickly exert curative effects,[52–55], which resulted the low bioavailability and high CL/F value under pathological conditions.

However, Cortex Moutan Carbon, the Processed product of Moutan Cortex (PMC), had the opposite effect of cooling blood and hemostatic. Our last article research found that PMC may promote the absorption of 5-HMF and inhibit oxypaeoniflorin, quercetin and 3, 8-Dihydroxy-2- methylchromone absorption in Blood-Heat and Hemorrhage Syndrome Model rat (BHH) as compared with the normal rats [56]. While the absorption of three components (3, 8-dihydroxy-2-methylchromone, benzoic acid, quercetin) was promoted and 5-HMF was inhibited in BHS-RMC. These revealed the opposite effective and processing mechanism of RMC.

Network analysis and molecular docking showed that the 4 compounds absorbed into the blood were capable of binding with F2, F10, F7, AKT1, MAPK14, MAPK10, PLAU and NOS3. According to the literature, F2, F7, F10 involved the coagulation system, which were directly involved in the mechanism of blood coagulation [39]. Tumor necrosis factor (TNF-α) could attack endothelial cells, which damaged vascular endothelial cells and caused abnormal function of coagulation factors[57]. HUVECs verification experiment had found that 4 compounds (paeonol, quercetin, paeoniflorin and oxypaeoniflorin) could significantly decline the content of F2, F7and F10 protein in TNF-α-induced HUVECs (excepting oxypaeoniflorin has no effect on F2). It has been previously reported that the coagulation system and the inflammatory system interact with each other. Not only does inflammation led to the activation of coagulation, but coagulation in turn affects inflammation [58]. MAPK10 and MAPK14 are members of the MAPK family that is widely involved in the inflammatory response and platelet activation. It plays a key role in the inflammatory response and thrombosis [59, 60]. Akt could be activated by a variety of platelet proteins, thus played an important role in platelet aggregation and hemostasis [61]. Those 4 compounds, paeonol, quercetin, paeoniflorin and oxypaeoniflorin may inhibit the expression of MAPK14 and MAPK10 to exert anti-inflammatory effect. In addition, oxypaeoniflorin could reduce the expression of AKT. According to the literatures, Paeoniflorin could inhibit the expression and secretion of inflammation-related proteins and chemokines by regulating p-MAPK. In addition, it could reduce platelet aggregation rate [62]. Paeonol and its metabolites had anti-inflammatory and antioxidant effects by blocking the MAPK/ERK/p38 signaling pathway [63]. Quercetin inhibited TNF-α-induced MAPK pathway activation, also had anti-angiogenic effects, which inhibited expression of proinflammatory factors and endothelin1[64–66]. These datas suggested that paeonol, quercetin, paeoniflorin and oxypaeoniflorin may be the active components of RMC for cooling and promoting blood circulation. And the mechanism of RMC against BHS syndrome may be acts on MAPK14 and MAPK10, which inhibited inflammatory pathways to regulate the expression of inflammatory, as well as interacted with F2, F10 and F7 regulated coagulation cascades pathway, which improve blood circulation, exerting anticoagulation and antiplatelet aggregation effects.

Conclusion

A network analysis integrated pharmacokinetics strategy was used to study the mechanism of action of nine components absorbed into blood after oral administration of RMC extracts in BHS and normal rats. The experimental results indicated that the mechanism of RMC for promoting blood circulation and cooling blood may be the regulation of the target genes, namely, F2, F10, F7, MAPK14 and MAPK10 through coagulation and inflammation pathways. It improves microcirculation, anti-inflammatory and inhibit platelet aggregation rate. The proposed pharmacokinetics integrated network analysis strategy in this experiment provides a combined method to systematically explore the absorption mechanism of multi-component drugs in the blood, clarifying the role of the nine components of RMC in the body. It lays the foundation for revealing the mechanism of RMC treatment of BHS.

Abbreviations

RMC
Raw Moutan Cortex
BHS
Blood-heat and blood stasis syndrome
UHPLC-DAD
Ultra -High -Pressure Liquid Chromatography coupled with Diode Array Detector
HUVECs
human umbilical vein endothelial cells
TCMSP
Traditional Chinese Medicine Systems Pharmacology Database and Analysis Platform
TTD
Therapeutic target database
PDB
Protein data bank
PPI
Protein-Protein Interactions
KEGG
Kyoto encyclopedia of genes and genomes
GO
Genome ontology.

Declarations

Acknowledgments

We sincerely thank Guangdong Pharmaceutical University for providing the platform for the experiment

Author Contributions

Qiuli Ye conceived and designed the study. Qiuli Ye wrote the paper draft; Jiang Meng, Ying Zhang and Qiuli Ye corrected the draft; Donghui Yan helped the first author prepared the materials of this paper. Yue Sun, Hui Cao and Shumei Wang contributed toward study design, experimental setup, results supervision, and manuscript correction.

Funding

This work was co-financed by grants from National Natural Science Foundation of China (No. 81473352, 82173973), the innovation project of Guangdong Province (2018KZDXM040) and the Guangzhou science and technology planning project (No. 201707010170).

Availability of data and materials

The datasets used and/or analyzed during the current study are available from

the corresponding author upon reasonable request.

Ethics approval and consent to participate

The animal care and experimental procedures used in the current study were approved by the Institutional Animal Experiment Center, Guangdong Academy of Medical Sciences (Certificate no. SCXK2013-0002)

Consent for publication

Not applicable.

Competing interests

The authors declare that the research was conducted in the absence of any commercial or financial relationships that could be construed as a potential conflict of interest.

Author details

[1] School of Traditional Chinese Medicine, Guangdong Pharmaceutical University /Key Laboratory of Digital Quality Evaluation of Chinese Materia Medica State Administration of Traditional Chinese Medicine (TCM) /Engineering Technology Research Center for Chinese Materia Medica Quality of Universities in Guangdong Province, Guangzhou, China.

2 College of Pharmacy, Jinan University, Guangzhou, China.

References

1. Bensky D, Gamble A: Chinese Herbal Medicine Materia Medica, Revised Edition. Washington; 1993.
2. Wang J. Study on the pharmacological effects of traditional Chinese medicine for promoting blood circulation and removing stasis. Medicine and Health (Abstract Edition). 2016; (4):00106–00106.
3. Gao C, Liu L, Hu A, Feng Y, Zhu L. Research progress on the pharmacological effects of traditional Chinese medicines for promoting blood circulation and removing blood stasis. Drug Evaluation Research. 2013;36(1):64–8.
4. Committee NP. Pharmacopoeia of the people's republic of China. Beijing: Chinese Medical Science and Technology Press; 2015.
5. Deng X, Yu J, Ding M, Zhao M, Xue X, Che C, Wang S, Zhao B, Meng J. Liquid chromatography-diode array detector-electrospray mass spectrometry and principal components analyses of raw and processed moutan cortex. Pharmacognosy Magazine. 2016;12(45):50–6.
6. Zhang L, Zhao B, Yuan J, et al: Comparative study on the activating blood effects of Moutan Cortex, Paeoniae Rubra and Radix Paeoniae Rubra on acute blood stasis model rats. *Chinese Herbal Medicine.* 2016; 47(15): 2676–2683.
7. Lu M, Pang L, Cheng P, Meng J, Wang S. Investigation of the integrated pharmacokinetics of the pharmacodynamic components of Moutan cortex and its correlation analysis with pharmacodynamics. Chin Experimental Pharmacol Magazine. 2019;25(15):148–54.
8. Qiu H, Zhang L, Zhu M, Zhang M, Chen J, Feng L, Jia X, Jacob J. Capture of anti-coagulant active ingredients from Moutan Cortex by platelet immobilized chromatography and evaluation of anticoagulant activity in rats. Biomed Pharmacother. 2017;95(2):235–44.
9. Hirai A, Terano T, Hamazaki T, Sajiki J, Saito H, Tahara K, Tamura Y, Kumagai A. Studies on the mechanism of antiaggregatory effect of Moutan Cortex. Thromb Res. 1983;31(1):29–40.
10. Chen J, Hou X, Wang G, Zhong Q, Liu Y, Qiu H, Yang N, Gu J, Wang C, Zhang L. Terpene glycoside component from Moutan Cortex ameliorates diabetic nephropathy by regulating endoplasmic reticulum stress-related inflammatory responses. J Ethnopharmacol. 2016;193:433–44.
11. Lu Y, Liu W, Zhang M, Deng Y, Jiang M, Bai G. The Screening Research of NF-κB Inhibitors from Moutan Cortex Based on Bioactivity-Integrated UPLC-Q/TOF-MS. Evid Based Complement Alternat Med. 2019;1–7.
12. Yun C, Choi Y, Jeong M. Moutan Cortex Radicis inhibits inflammatory changes of gene expression in lipopolysaccharide-stimulated gingival fibroblasts. J Nat Med. 2013;67(3):576–89.
13. Zhang Y, Wu X, Wang X, Zeng Y, Liao Y, Zhang R, Zhai F, Zeng Z. Grey Relational Analysis Combined With Network Pharmacology to Identify Antioxidant Components and Uncover Its Mechanism From Moutan Cortex. Front Pharmacol. 2021;12:748501.
14. Zhang M, Feng L, Gu J, Ma L, Qin D, Wu C. The attenuation of 3 Moutan Cortex on oxidative stress for renal injury in AGEs-induced mesangial cell 4 dysfunction and streptozotocin-induced diabetic nephropathy rats. Oxid Med Cell 5 Longev. 2014; (1), 463815.

15. Chen J, Zhang M, Zhang L, Zhao D, Feng L, Jia X. Protective effects and mechanism of glycosides/phenol component of Moutan Cortex on renal injury of diabetic nephropathy rats. Zhongguo Zhong Yao Za Zhi. 2016;41(11):1990–8.
16. Dan H, Zhang L, Qin X, Peng X, Wong M, Tan X, Yu S, Fang N. Moutan cortex extract exerts protective effects in a rat model of cardiac ischemia/reperfusion. Can J Physiol Pharmacol. 2016;94(3):245–50.
17. Cao C. Advances on chemical constituents of Chinese Moutan Cortex. Guangzhou Chem Ind. 2013;41(12):41, 44–45, 51.
18. Song L: The three-dimensional structure and free radical scavenging effect of two monoterpenes in Moutan Cortex. *Foreign Medicine (Chinese Medicine and Chinese Medicine Volume)*. 2002.
19. Jiang L, Zhang Y, Wang C, Zhao D. Research progress in the pharmacological activity of paeonol, an active ingredient in Cortex Moutan. Mod Diagnosis Treat. 2016;27(22):4223–4.
20. Wang W, Wang X, Zhang X. Study on anti platelet aggregation activity of Pinus massoniana Needles. Chin J Hosp Pharm. 2008;28(3):190–4.
21. Karimi-Khouzani O, Heidarian E, Amini SA. Anti-inflammatory and ameliorative effects of gallic acid on fluoxetine-induced oxidative stress and liver damage in rats. Pharmacol Rep. 2017;69(4):830–5.
22. Kleemann R, Verschuren L, Morrison M, Zadelaar S, Erk VMJ, Wielinga PY, Kooistra T. Anti-inflammatory, anti-proliferative and anti-atherosclerotic effects of quercetin in human in vitro and in vivo models. Atherosclerosis. 2011;218(1):44–52.
23. Sanae F, Miyaichi Y, Hayashi H. Endothelium-dependent contraction of rat thoracic aorta induced by gallic acid. Phytotherapy Res. 2003;17(2):187–9.
24. Ye JF, Duan HL, Yang XM, Yan WM, Zheng XX. Anti-thrombosis effect of paeoniflorin: Evaluated in a photochemical reaction thrombosis model in vivo. Planta Med. 2001;67:766–8.
25. Yang X, Xue X, Lin Y, Huang Q, Mo M, Wang S, Meng J. Chemical constituents from the Moutan Cortex charcoal and their potential coagulation activities. J Chin Pharm Sci. 2018;27(9):608–16.
26. Ding MJ, Deng XM, Meng J, Zhu Q, Wang S, Liang S. Simultaneous Assay of Three Kinds of Monoterpene Paeoniflorin Class and Paeonol in Moutan Cortex by Quantitative Analysis of Multi-components by Single Marker. Chinese Journal of Experimental Traditional Medical Formulae. 2014.
27. Yang G, Zhang C, Li P, Dong F. Chemical Fingerprinting and Quantitative Analysis of Cortex Moutan From Different Tree Peony Cultivars Using HPLC-ESI/MS. Nat Prod Commun. 2020;15(11):1934578X2097351.
28. Wang Z, Xiao P, Jie S, Pei L, Liu S, Fan Y, Liu H, Wu F, He C, Chen F. Research on Quality Markers of Moutan Cortex: Quality Evaluation and Quality Standards of Moutan Cortex. Chin Herb Med. 2017;9(004):307–20.
29. Wu X, Chen H, Chen X, Hu Z. Determination of paeonol in rat plasma by high-performance liquid chromatography and its application to pharmacokinetic studies following oral administration of Moutan cortex decoction. Biomed Chromatogr. 2003;17(8):504–8.
30. Wu H, Zhu Z, Zhang G, Zhao L, Zhang H, Zhu D, Chai Y. Comparative pharmacokinetic study of paeoniflorin after oral administration of pure paeoniflorin, extract of Moutan Cortex and Shuang-Dan prescription to rats. J Ethnopharmacol. 2009;125(3):444–9.
31. Li C. Studies on the pharmacokinetics of multiple components of traditional Chinese medicine: ideas and methods. Chin J Chin Materia Med. 2017;42(4):607–17.
32. Sun H, Wu F, Zhang A, Wei W, Han Y, Wang X. Profiling and identification of the absorbed constituents and metabolites of schisandra lignans by ultra-performance liquid chromatography coupled to mass spectrometry. Biomed Chromatogr. 2013;27:1511–9.
33. Wang X. Progress and future developing of the serum pharmacochemistry of traditional Chinese medicine. Asia Pac Traditional Med. 2006;31(10):789–92.
34. Ding M, Ma W, Wang X, Chen S, Zou S, Wei J, Yang Y, Li J, Yang X, Wang H. A network pharmacology integrated pharmacokinetics strategy for uncovering pharmacological mechanism of compounds absorbed into the blood of Dan-Lou tablet on coronary heart disease. J Ethnopharmacol. 2019;242:112055.
35. Xia Z, Lv L, Di X, Xue J, Gao Z, Zhang G, Zhang H. The compatibility of six alkaloids in ermiao pill explored by comparative pharmacokinetic and network pharmacological study. Biomedical Chromatogr. 2019;33(5):e4509.

36. Tian Y, Yang ZF, Li Y, Qiao Y, Yang J, Jia Y, Wen A. Pharmacokinetic comparisons of hydroxysafflower yellow A in normal and blood stasis syndrome rats. J Ethnopharmacol. 2010;129(1):1–4.
37. Liu J, Zhang L, Ding A, Yao Y, Shan M, Yu B, Yao W. Establishment of blood-heat and hemorrhage syndrome rat model based on Traditional Chinese Medicine characteristics. Chin Pharmacol Bull. 2012;28(9):1319–24.
38. Wang X, Shen Y, Wang S, Li S, Zhang W, Liu X, Lai L, Pei J, Li H. PharmMapper 2017 update: a web server for potential drug target identification with a comprehensive target pharmacophore database. Nucleic Acids Research. 2017;45:356–60.
39. She G, Lin Y, Wu D. Network pharmacology of the anticoagulant effects of traditional Chinese medicine. Chin J Experimental Formulas. 2014;20(16):224–30.
40. Yang K, Zeng L, Ge A, Ge J, Long Z, Bao T. Based on network pharmacology to explore the molecular mechanism of peach kernel-safflower medicine for promoting blood circulation and removing blood stasis. World Sci Technology-Modernization Traditional Chin Med. 2018;20(12):124–32.
41. Lv M, Wang T, Tian X, Shi X, Fan G, Zhang Y, Zhu Y. Anti-inflammatory and antithrombotic effects of commonly used Chinese medicines for promoting blood circulation and removing blood stasis revealed by network pharmacological analysis. Acta Pharm Sci. 2015;50(9):1135–41.
42. Ouyang L, Hu X, Niu M, Gao W, Cheng Y, Wang J. Study on the mechanism of action of leeches for promoting blood circulation and removing blood stasis based on network pharmacology. Chin J Chin Materia Med. 2018;43(9):1901–6.
43. Huang M, Zhang Y, Ren Z, Qiao Y. Network pharmacology approach to explore the mechanism of promoting blood circulation and removing blood stasis in the treatment of coronary heart disease. World Sci Technology: Modernization Traditional Chin Med. 2012;14(5):1969–75.
44. Zou C, Hong G, Yan H. Network pharmacology predicts the anti-myocardial ischemia-reperfusion injury mechanism and validation study of Gualou. Chin J Pharmaceuticals. 2019;54(7):1234–40.
45. Xu N, Wang L, Sun R, Huang X, Zhang C, Shi H. Based on the integrated pharmacology platform to explore the molecular mechanism of anti-thrombosis and anti-platelet aggregation. Chin J Experimental Pharmacol. 2019;25(5):200–8.
46. Liu M, Wu D, Li J, Hou N, Zhang Y, Qiao Y. Study on the relationship between bitterness, taste and effect of traditional Chinese medicine for promoting blood circulation and removing blood stasis based on drug combination. Chin J Chin Materia Med. 2019;44(2):218–23.
47. Li J, Wu D, Hou N, Liu M, Zhang Y, Qiao Y. Study on the relationship between warming and bitter liver and cold and bitter liver based on the effect of promoting blood circulation and removing blood stasis. Chin J Chin Materia Med. 2019;44(2):14–9.
48. Jain AN. Scoring noncovalent protein-ligand interactions: A continuous differentiable function tuned to compute binding affinities. J Computer-Aided Mol Des. 1996;10(5):427–40.
49. Guo L, Guo W. The pharmacokinetics of paeonol preparations in different administration routes in rabbits. J Liaoning Med Coll. 2007;28(4):4–8.
50. Ying X, Zhou Y, Wong H, Xu Z, Jiang L. Study on the pharmacokinetics and metabolism of paeonol in rats treated with pure paeonol and an herbal preparation containing paeonol by using HPLC–DAD-MS method. J Pharm Biomedical Anal. 2007;46(4):748–56.
51. Li H, Wang S, Zhang B. Research progress in the pharmacological activity and pharmacokinetics of paeonol. Asia-Pacific Traditional Medicine. 2010;6(2):110–2.
52. Zhang S, Guo J, Kang A, Di L. Research progress of gut microbiota on deglycosylation metabolism of glycosides in traditional Chinese medicin. Chin J Chin Materia Med. 2013;38(10):1459–66.
53. Liu Z, Jiang Z, Liu L, Hu M. Mechanisms responsible for poor oral Bioavailability of paeoniflorin: Role of intestinal disposition and interactions with sinomenine. Phamarceutical Reaserch. 2006;23(12):2678–780.
54. Takeda S, Isono T, Wakui Y, Mizuhara Y, Amagaya S, Maruno M, Hattori M. In-vivo assessment of extrahepatic metabolism of paeoniflorin in rats:relevance to intestinal floral metabolism. J Pharm Pharmacol. 1997;49(1):35–9.
55. Ju-Xiu H, Emi G, Teruaki A, Tadato T. Interaction between Shaoyao–Gancao–Tang and a laxative with respect to alteration of paeoniflorin metabolism by intestinal bacteria in rats. Phytomedicine. 2006;14(7):452–9.

56. Ye Q, Cheng P, Yan D, Sun Y, Zhang Y, Cao H, Wang S, Meng J. Nine absorbed components pharmacokinetic of raw and processed Moutan Cortex in normal and blood-heat and hemorrhage syndrome model rats. Biomedical chromatography: BMC. 2020;34(12):e4963.
57. Zhang Z. Interaction between systemic infection, inflammation and blood coagulation. In: *Intensive Medicine——2011: People's Medical Publishing House: 2011*. 2011: 351–356.
58. Teradagimenez B, Nevescezarette G, Sousabomfim AD, Marcelomonteiro W, Aureliosartim M. Role of crotoxin in coagulation: novel insights into anticoagulant mechanisms and impairment of inflammation-induced coagulation. Journal of Venomous Animals and Toxins including Tropical Diseases. 2020; 26(5).
59. Li M, Zhou Z, Sun X, Zhang X, Zhu XJ, Jin SG, Gao YT, Jiang Y, Gao YQ. Hepatitis B core antigen upregulates B7-H1 on dendritic cells by activating the AKT/ERK/P38pathway:A possible mechanism of hepatitis B virus persistence. Lab Invest. 2016;96(11):1156–64.
60. Kim H, Kim K, Seo K, Lee H, Im S. PTEN/MAPK pathways play a key role in platelet-activating factor-induced experimental pulmonary tumor metastasis. Febs Lett. 2012;586(24):4296–302.
61. Crawley J, Zanardelli S, Chan K, Lane C, Lane D. The central role of thrombin in haemostasis. J Thromb Haemostasis. 2007;1(1):95–101.
62. Hong X, Li L, Guo D, Yang Z, Yan J. Paeoniflorin can improve the permeability of cardiac microvascular endothelial cells by regulating Src/vascular endothelial-cadherin pathway. Chinese Critical Care Medicine. 2020; (01):83–87.
63. Jin X, Wang J, Xia Z, Shang CH, Zhao F. Anti-inflammatory and Anti-oxidative Activities of Paeonol and Its Metabolites Through Blocking MAPK/ERK/p38 Signaling Pathway. Inflammation. 2016;39(1):434–46.
64. Yang B, Zheng CY, Zhang R, Zhao C, Li S, An Y. Quercetin efficiently alleviates TNF-α-stimulated injury via STAT1 and MAPK pathway in H9c2 cells: a protective role of quercetin in Myocarditis. Journal of Cardiovascular Pharmacology. 2021; publish ahead of print.
65. Hong-Chao P, Qiong, Jiang Y, Mei YJin-Ping. Yu-Kun, Cui: Quercetin promotes cell apoptosis and inhibits the expression of MMP-9 and fibronectin via the AKT and ERK signalling pathways in human glioma cells. Neurochemistry Int. 2015;80:60–71.
66. Rashidi M, Mohammadzadeh G, Sanaei A. Quercetin Synergistically Potentiates the Anti-Angiogenic Effect of 5- Fluorouracil on HUVEC Cell Line. 2021.

Figures

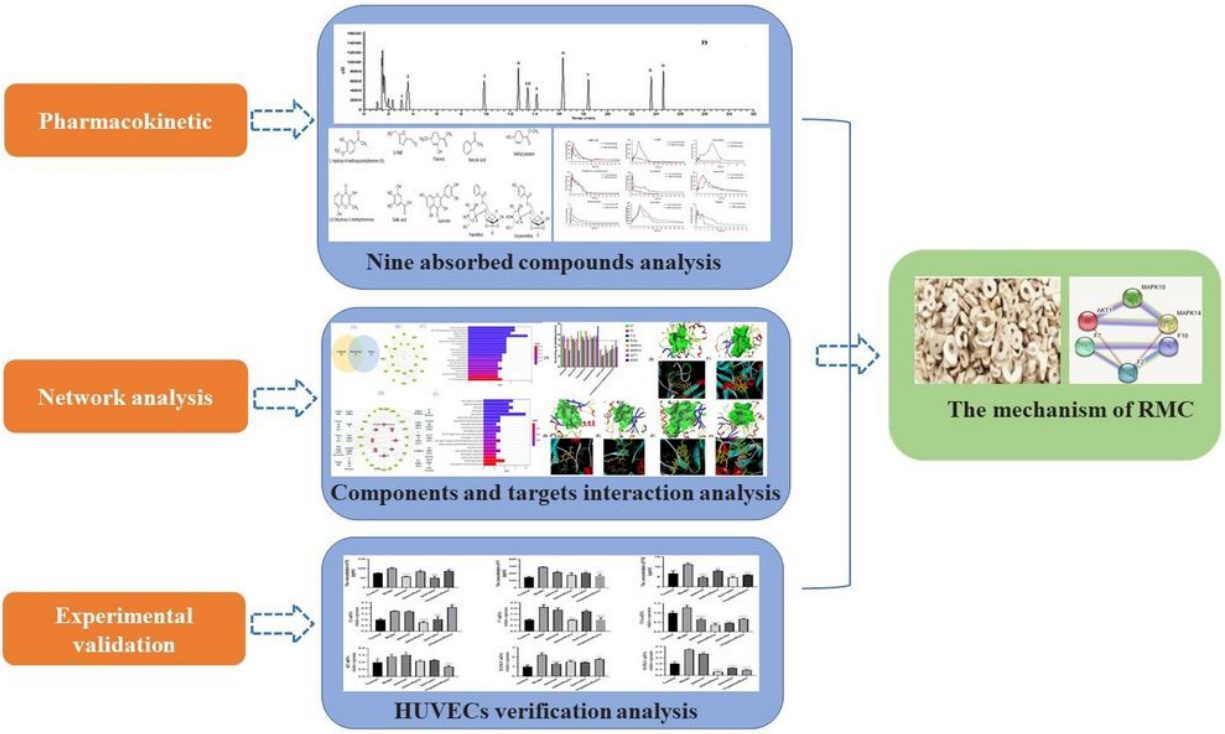

Figure 1

Flow chart of integrating pharmacokinetics and network analysis to investigate the mechanism of Moutan Cortex in Blood-Heat and blood Stasis Syndrome

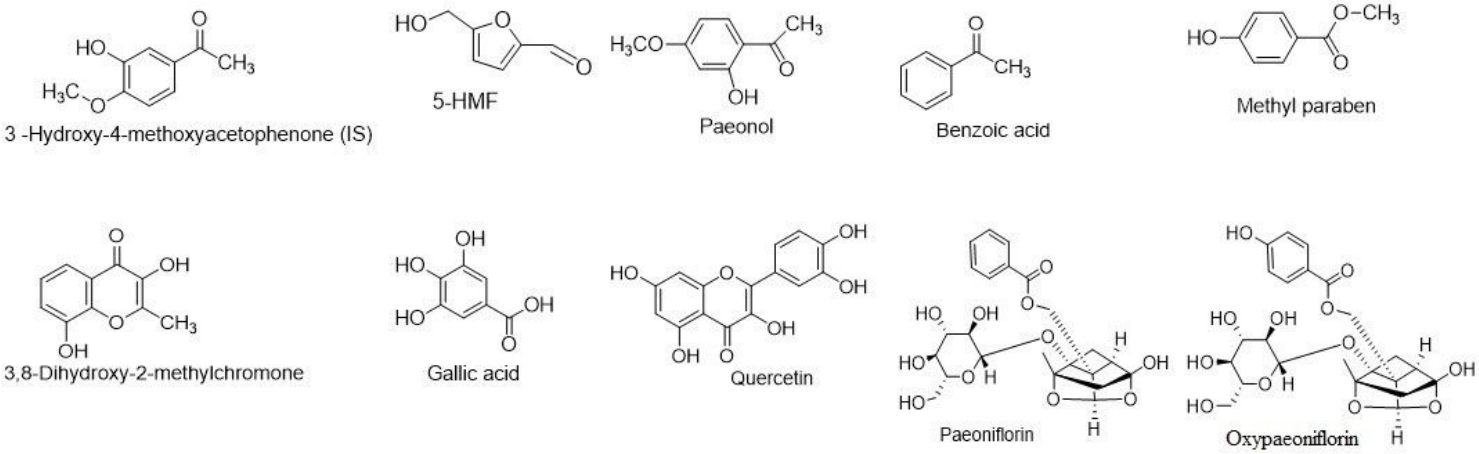

Figure 2

Chemical structure of the analytes and IS.

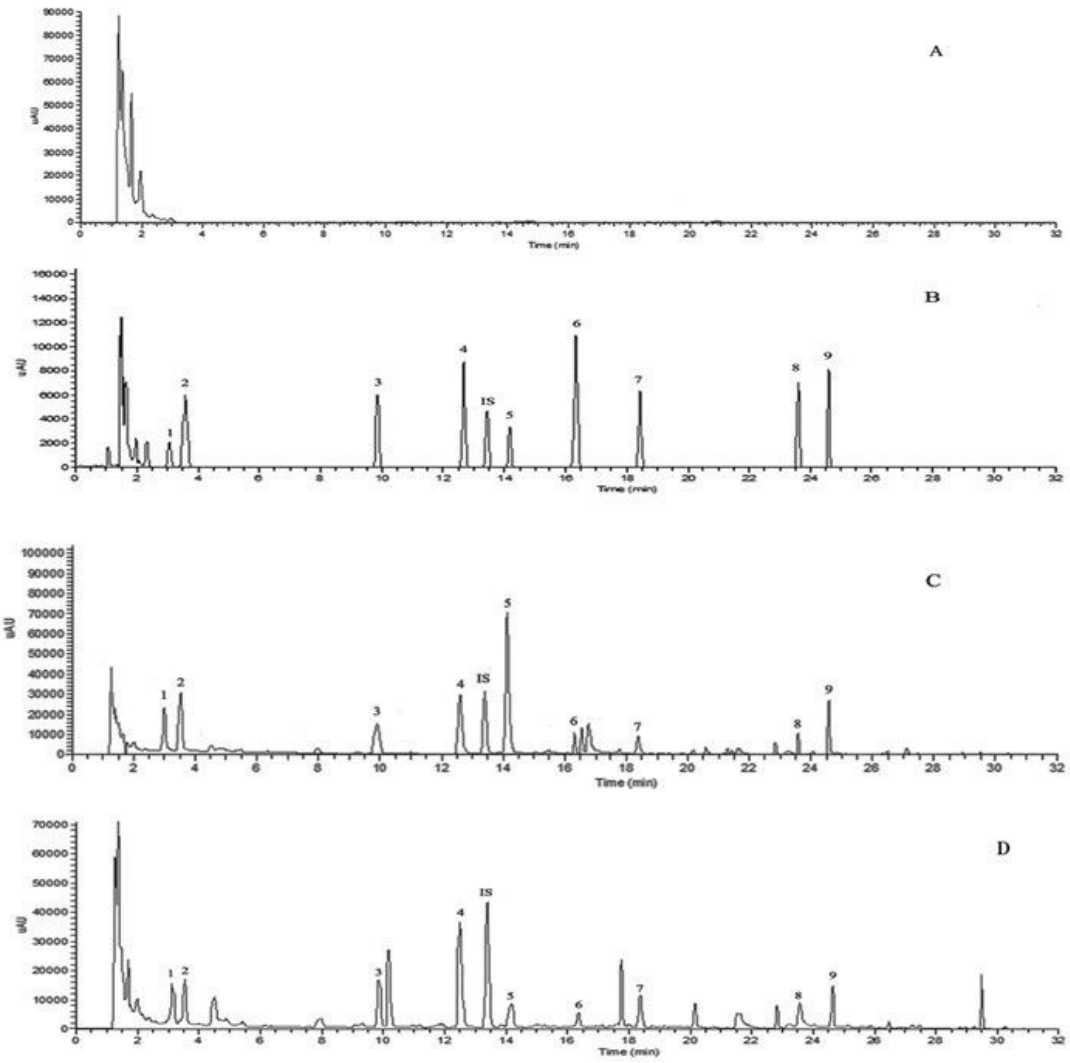

Figure 3

UHPLC chromatograms of rats serum samples: (A) blank serum; (B) blank serum spiked with the nine analytes and IS; (C) serum sample of N-RMC at 1 h;(D) serum sample of BHS-RMC at 1 h; Standards: (1) 5-HMF; (2) Gallic acid; (3) Oxypaeoniflorin; (4) Paeoniflorin; (5) 3,8-Dihydroxy-2-methylchromone; (6) Benzoic acid; (7) Methyl paraben; (8) Paeonol; (9) Quercetin; (IS) 3-Hydroxy-4-methoxyacetophenone.

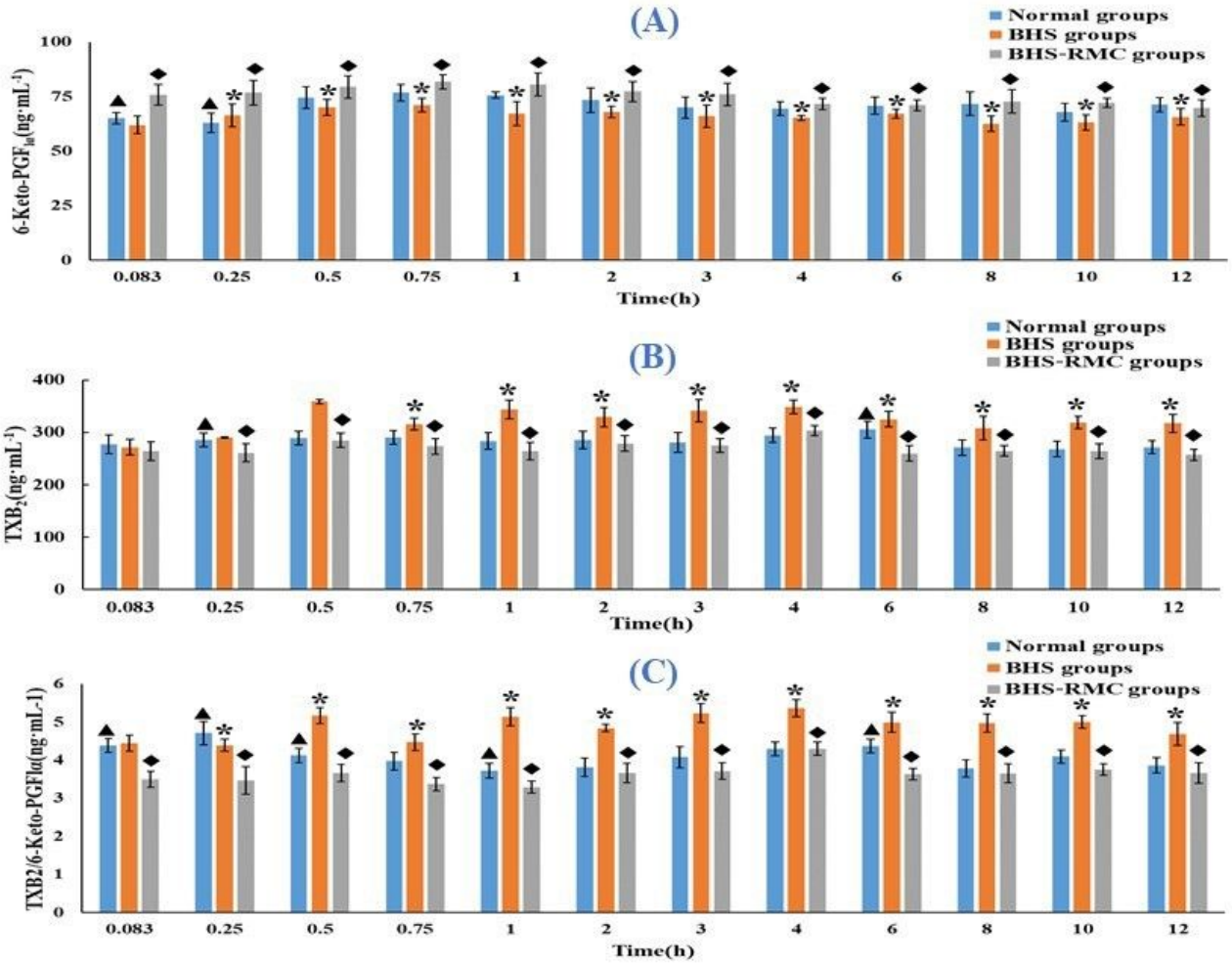

Figure 4

6-Keto-PGFIα (A), The TXB2 (B) and TXB2/6-Keto-PGFIα(C) value of rats in each group at the same time"*" means there is a significant difference between the BHS model group and the Normal group (P<0.05); "" means the BHS group is significantly different from the BHS- RMC group (P<0.05); "▲" means BHS- RMC and Normal Significant difference between groups (P<0.05).

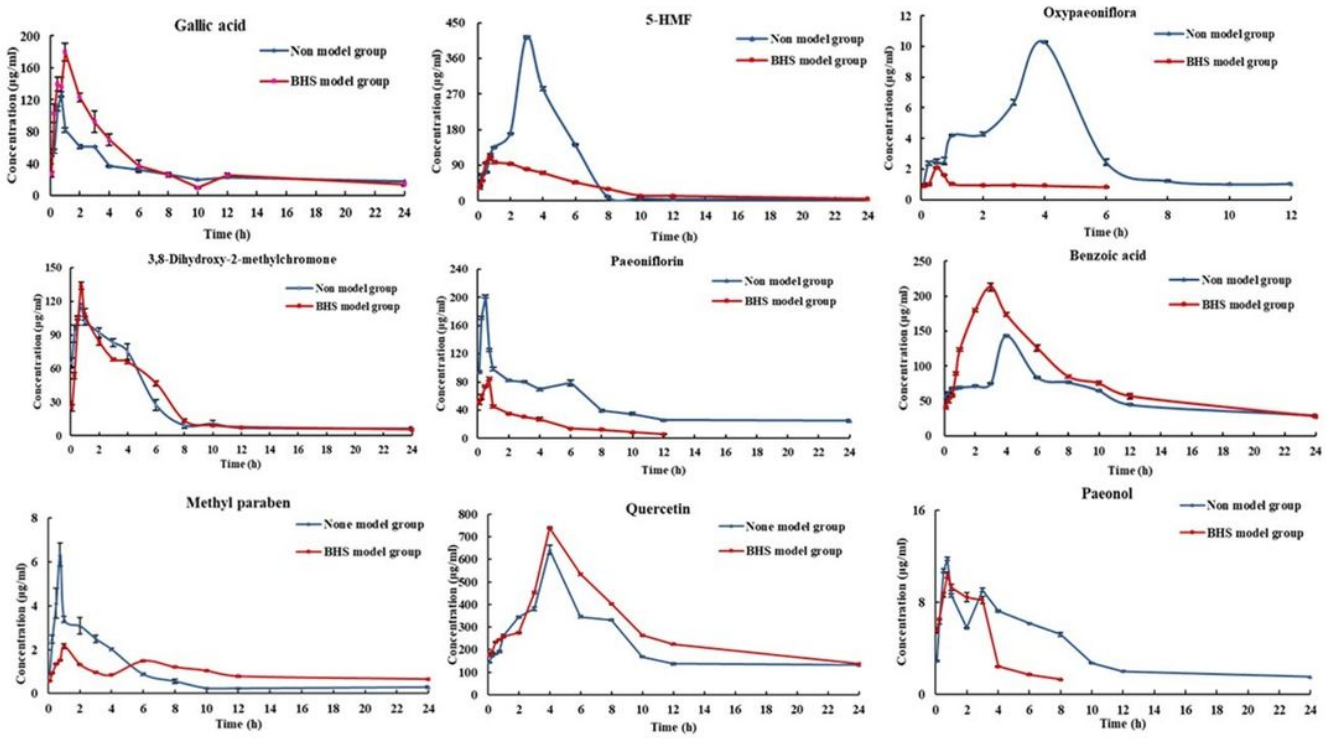

Figure 5

The mean plasma concentration time profiles of Gallic acid, 5-HMF, Oxypaeoniflorin,3,8-Dihydroxy-2-methylchromone, Paeoniflorin, Benzoic acid, Methylparaben, Quercetin and Paeonol after oral administration of RMC Extract (n=6, mean±SD)

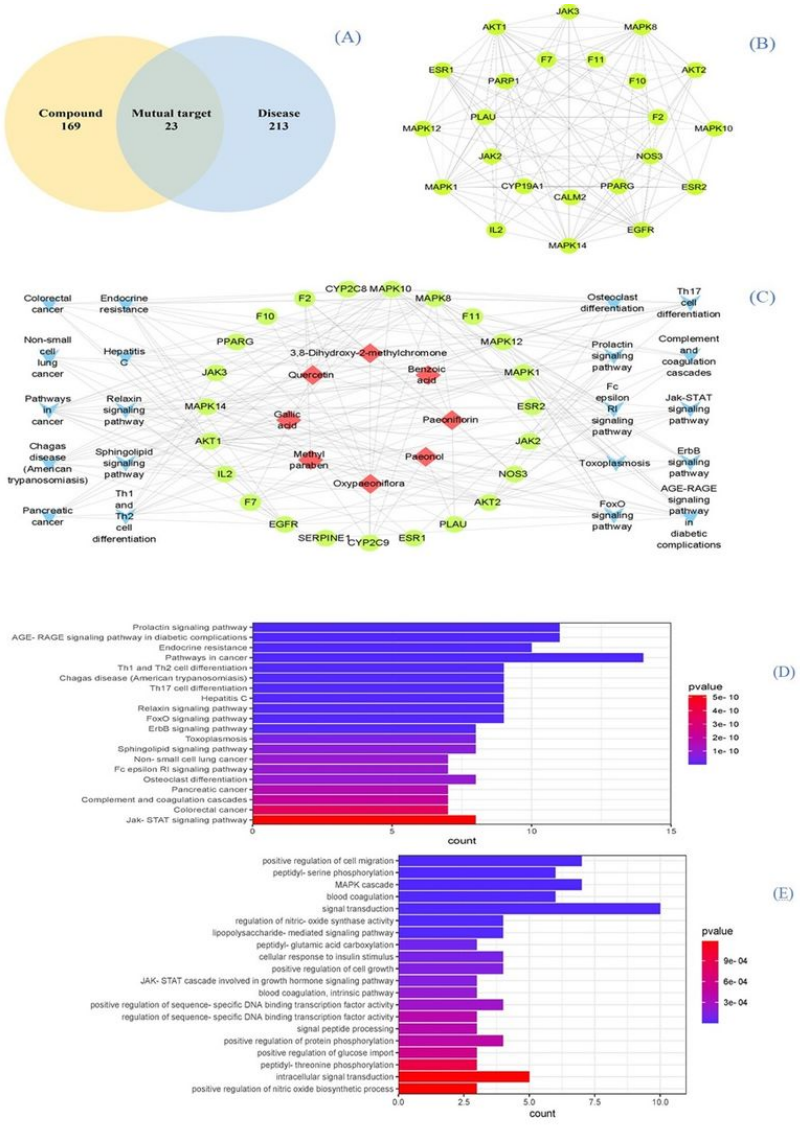

Figure 6

Network analysis of the nine compounds absorbed into the blood in treating BHS syndrome. (A) Targets attribution among the RMC and BHS syndrome. (B) Protein-protein interaction network of hub targets obtained from STRING database and constructed by Cytoscape, target gene indicated by green circle; (C) Top 20 KEGG pathway enrichment entries ($p < 0.05$) (D) Ingredients -target-pathway network. Labels Red diamonds, ingredients; green circles, protein targets; Blue V, Pathway; gray lines, compound–target pathway interactions. (E) Top 20 GO enrichment entries ($p < 0.05$).

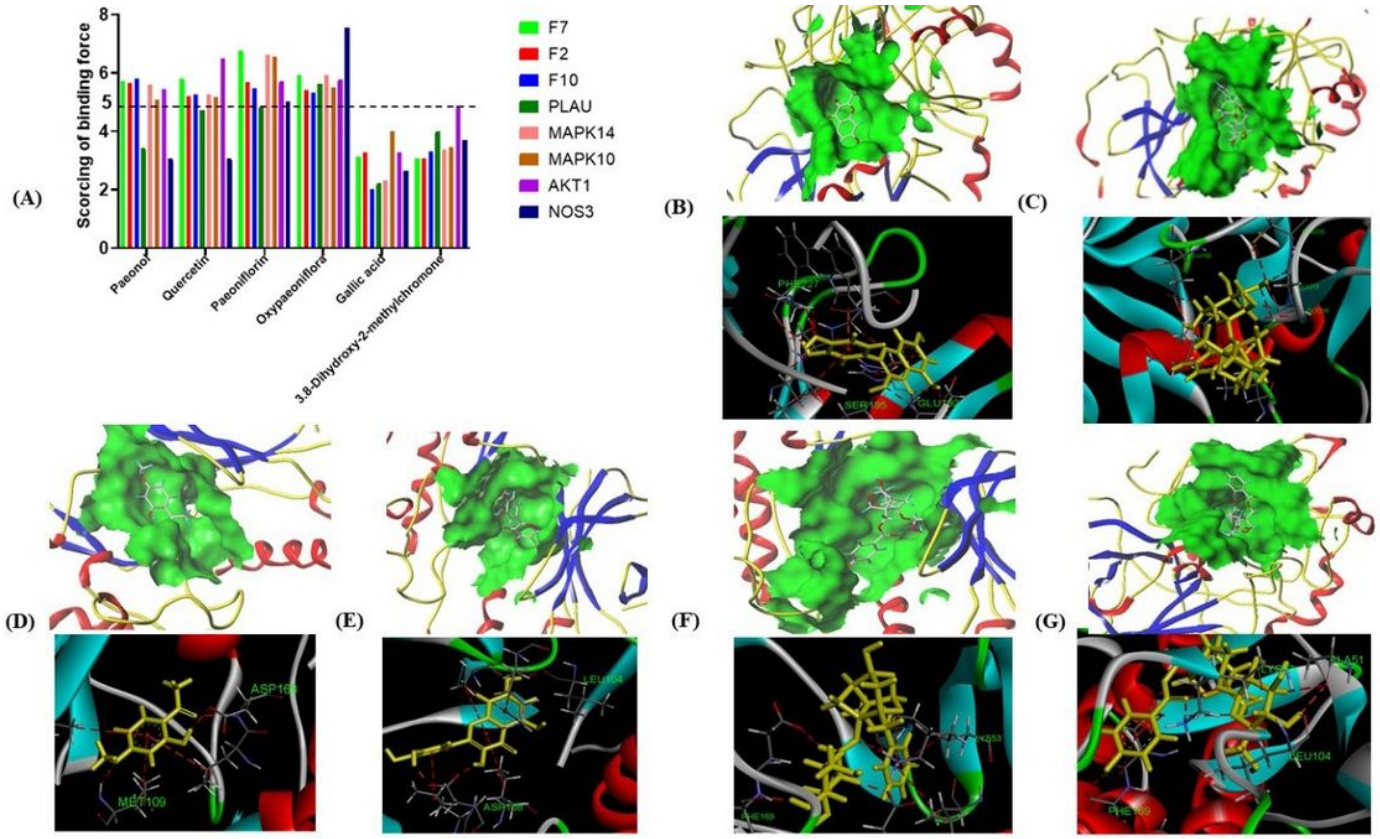

Figure 7

Binding compounds of RMC interacting with target proteins. (A) The scoring of binding force between 6 compounds and 8 proteins. (B-G) Binding studies of compounds –targets interactions. Molecules are represented by a yellow stick model, the hydrogen bonds are represented by a red dotted line. quercetin (B)paeoniflorin(C) within the F2(3tu7) kinase active site respectively. paeonol (D), quercetin(E), Paeoniflorin (F), oxypaeoniflora(G) within the MAPK14(ID =1a9u) kinase active site respectively.

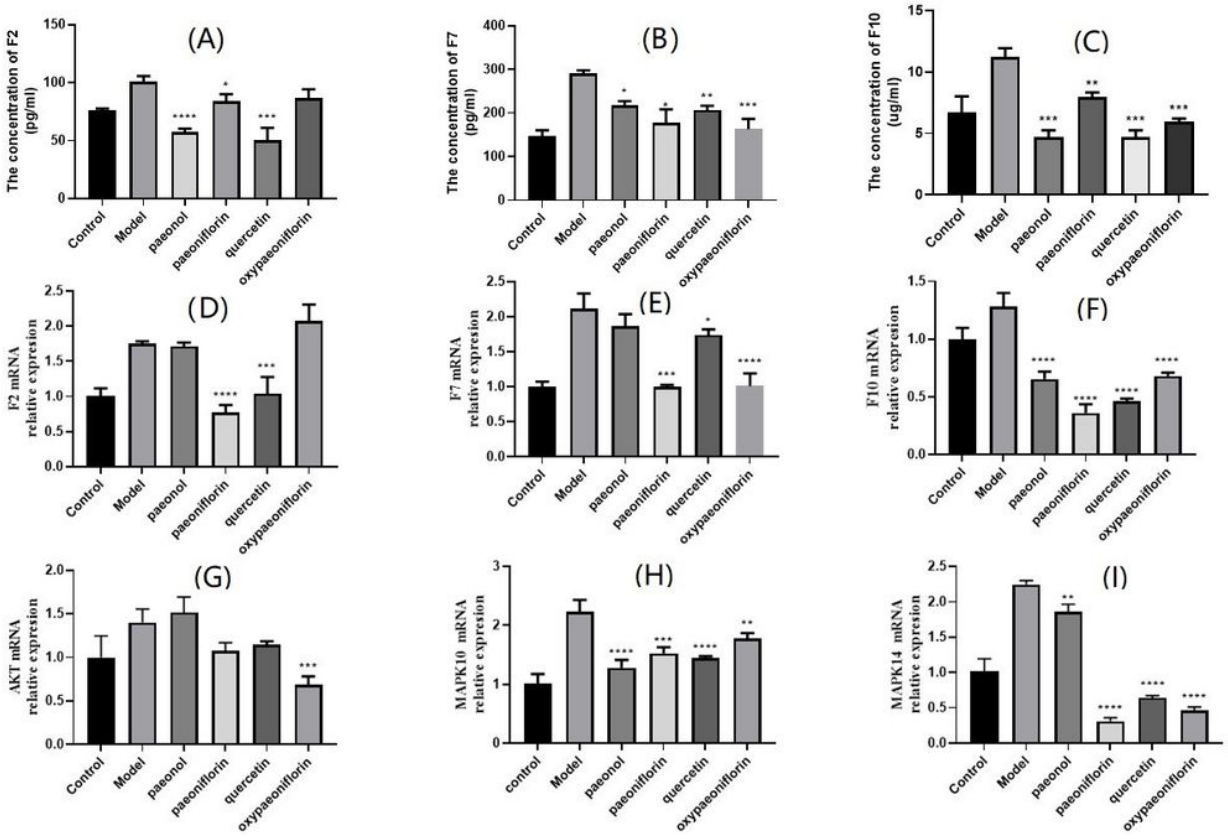

Figure 8

Production of F2 (A), F7(B) and F10 (C) was determined by ELISA. Protein expression of F2(D) F7 (E), F10 (F), AKT(G), MAPK14 (H) and MAPK10 (I) was determined by RT-qPCR. *p < 0.05, **p < 0.01, ***p < 0.001, ****p < 0.0001 versus Model group.

Supplementary Files

This is a list of supplementary files associated with this preprint. Click to download.

- GA.jpg
- supplementary.docx